analytical chemistry

Article

pubs.acs.org/ac

Direct Electron Transfer of Glucose Oxidase-Boron Doped Diamond Interface: A New Solution for a Classical Problem

Yan-Feng Bai,[†] Tai-Bin Xu,[†] John H. T. Luong,[‡] and Hui-Fang Cui*[,†]

[†]School of Life Sciences, Zhengzhou University, 100[#] Science Avenue, Zhengzhou 450001, P.R. China

[‡]Innovative Chromatography Group, Irish Separation Science Cluster (ISSC), Department of Chemistry and Analytical, Biological Chemistry Research Facility (ABCRF), University College Cork, Cork, Ireland

Supporting Information

ABSTRACT: A planar boron-doped diamond (BDD) electrode was treated with KOH and functionalized with 3-aminopropyltriethoxysilane (APTES) to serve as a biosensing platform for biomolecule immobilization with glucose oxidase (GOx) as a test model. The free amino groups of GOx and APTES were cross-linked by glutaraldehyde (X), a bifunctional chemical to form a stable enzyme layer (GOx-X-APTES) on BDD. Micrographs obtained by scanning electron microscopy revealed that a mesoporous structure uniformly covered the BDD surface. Cyclic voltammetry of GOx immobilized showed a pair of well-defined redox peaks in neutral phosphate buffer solution, corresponding to the direct electron transfer of GOx. The apparent heterogeneous electron transfer rate constant of the immobilized GOx was estimated to be 8.85 ± 0.47 s^{-1}, considerably higher than the literature reported values. The determination of glucose was carried out by amperometry at −0.40 V, and the developed biosensor showed good reproducibility and stability with a detection limit of 20 μM. Both ascorbic and uric acids at normal physiological conditions did not provoke any signals. The dynamic range of glucose detection was further extended by covering the enzyme electrode with a thin Nafion layer. The Nafion/GOx-X-APTES/BDD biosensor showed excellent stability, a detection limit of 30 μM, a linear range between 35 μM and 8 mM, and a dynamic range up to 14 mM. Such analytical performances were compared favorably with other complicated sensing schemes using nanomaterials, redox polymers, and nanowires. The APTES-functionalized BDD could be easily extended to immobilize other redox enzymes or proteins of interests.

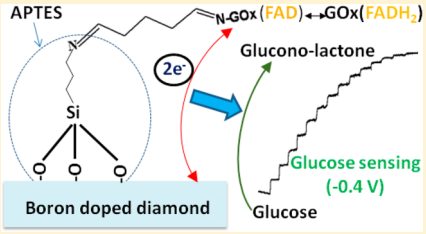

Direct electron transfer (DET) of immobilized glucose oxidase (GOx), possessing bioelectrocatalytic activity is a prerequisite for applications as the third generation enzyme biosensors and biofuel cells. However, the flavin adenine dinucleotide (FAD) active redox center of GOx is deeply embedded within a protective protein shell. Therefore, DET of GOx, like some other redox enzymes, is extremely difficult. As an intensive research subject, several attempts with different degrees of success have been reported to overcome the long distance between the redox-active cofactor and the electrode surface.[1−8] Nanomaterials such as carbon nanotubes[1,2] and graphene[3,4] have been extensively used to modify the electrode surface to promote DET. Attachment of mediators to the enzyme surface or to a surrounding redox polymer is another successful strategy.[5,6] An elegant approach of bridging the redox-active center of an enzyme and an electrode via gold nanoparticles was reported and this scheme can be considered as an electron-mediating two-electron "relay".[7] Recently, genetic modification of GOx with a free thiol group near its active site was described.[8] This approach facilitates the site-specific attachment of a maleimide-modified gold nanoparticle to the enzyme, effecting direct electrical communication between the conjugated enzyme and an electrode. In general, the above-mentioned approaches involve complicated and high-cost procedures, including chemical synthesis, genetic modification, and/or reconstitution of native enzymes around modified cofactors.

Boron-doped diamond (BDD) electrodes have inspired considerable attention as an excellent functional material compared to conventional carbon-based and metal electrodes.[9−12] BDD electrodes with different surface structures on various substrates have been successfully synthesized by chemical vapor deposition and are now commercially available. The BDD surface is less vulnerable to surface fouling and exhibits a wide potential window for important applications that are impossible with conventional electrodes. With a low background current, high reproducibility, excellent stability, good biocompatibility, and amenability for functionalization, BDD is a good sensing material for the fabrication of chemical and biosensors. Metal complexes and metal oxides have been decorated on diamond electrodes to improve the electrocatalysis of metal compounds.[13−15] To date, only a few BDD-based enzyme electrodes have been reported in the literature: (i) a glucose biosensor developed by connecting glucose oxidase (GOx) to BDD via ferrocene-based electron transfer relays,[16] (ii) peroxidase- and heme peptide-modified BDD electrodes for sensing of hydrogen peroxide,[17] (iii) an alcohol

Received: January 17, 2014
Accepted: April 26, 2014
Published: April 26, 2014

   dx.doi.org/10.1021/ac501143e | *Anal. Chem.* 2014, 86, 4910−4918

biosensor using BDD and alcohol dehydrogenase,[18] (iv) a tyrosinase-modified electrode for detection of estrogenic phenol derivatives, and (v) GOx entrapment in an electropolymerized film on Pt nanoparticle modified BDD.[19] Some other BDD-based biosensors can be found from a recent review.[20]

3-Aminopropyltriethoxysilane (APTES) has been used as a surface modification agent for immobilization of biomolecules on various bioanalytical platforms.[21] Functionalization of electrode surfaces by organic silane monolayers is of importance for numerous applications ranging from molecular electronics to chemical/biological sensing. However, the use of APTES for immobilization of GOx on BDD to fabricate a glucose biosensor has not been addressed.

This paper describes a simple procedure for stably immobilizing GOx on the surface of the BDD electrode, and realizing DET between the FAD center of GOx and the electrode, by using APTES-glutaraldehyde conjugate as a molecular wire to form electron tunnelling between the FAD center and BDD. The DET features of the wired enzyme are determined. Amperometric responses of the GOx electrode to glucose are illustrated in both aerated and deaerated buffer solution to address whether the signal response to glucose can be attributed to DET (i.e., bioelectrocatalysis). The performance characteristics of the biosensor with respect to detection limit, linearity, and electroactive interferences are presented and discussed in detail, and the applicability of the biosensor to detect human serum glucose is evaluated.

EXPERIMENTAL SECTION

Chemicals and Materials. GOx (EC 1.1.3.4, Type X-S from *Aspergillusniger*, G7141), D-glucose, 3-aminopropyltriethoxysilane (APTES) (purity: 98%), glutaraldehyde (70%), Nafion (5%), flavin adenine dinucleotide (FAD), ascorbic acid, and uric acid were purchased from Sigma-Aldrich (St. Louis, MO). Other remaining chemicals were obtained from Sinopharm Chemical Reagent (Shanghai, China). All chemicals were of analytical grade and used as received. Glucose solution was prepared in a 0.01 M neutral phosphate buffered solution (PBS, pH 7). The glucose solution was stored overnight at room temperature (RT), while other solutions were freshly prepared just before use. Deionized (DI) water obtained from a Millipore water system was used throughout the experiment. Purified nitrogen with purity of 99.99% was obtained from Zhengzhou Keyi Industrial Gas (Zhengzhou, China).

Apparatus and Instrumentation. Scanning electron microscopy (SEM), energy dispersive spectroscopy (EDX), and Fourier transform-infrared spectroscopy (FT-IR) were used to evaluate the surface morphology, composition, and structure of the electrodes prior to and after modification. A Hitachi SEM (S-2600N, Tokyo, Japan) was used for topographical analysis of the electrodes. The SEM was equipped with an EDX spectrometer (Inca-X-act LN2-free analytical silicon drift detector, Oxford Instruments, U.K.). The SEM/EDX system was operated with a high vacuum mode at 10−20 kV, emission current of 60−80 μA, and a working distance of 3−20 mm with tilt angle of 30° for elemental analysis. The EDX has software with a database of reference spectra for elemental analysis, compositional nanoanalysis, and mapping. In order to improve the SEM imaging of the nonconducting modifying layer, a very thin nanometric Au layer was sputtered on the modified BDD surface using a Cressington Sputter Coater Model 108 (Cressington Scientific Instruments, England, U.K.). Attenuated total reflectance FT-IR (ATR-FT-IR) spectra were collected from 4000 to 600 cm^{-1} for 64 scans and 4 cm^{-1} resolution, using a zinc selenide (ZnSe) crystal on a Bruker Tensor 27 FT-IR spectrophotometer.

All electrochemical measurements were carried out at RT on CHI 660C electrochemical workstation (Shanghai Chenhua Instrument, CHI, China) with a three-electrode system: the working electrode, Pt counter electrode, and a Ag/AgCl/KCl (3 M) reference electrode. Unless otherwise indicated, all electrochemical measurements were performed in the presence of oxygen dissolved in a reaction mixture under ambient air. For some specific experiments carried out in the nitrogen-saturated or oxygen-saturated buffer, the reaction mixture was bubbled with pure nitrogen or pure oxygen for 30 min just before the experiments, and covered with a nitrogen or oxygen blanket, respectively, and maintained above the liquid during the course of the measurement.

Electrode Preparation and Enzyme Immobilization. The BDD electrode (3 mm in diameter, 0.1% boron-doped diamond) was purchased from Windsor Scientific (Slough, Berkshire, U. K.) and used for enzyme immobilization. The BDD was polished consecutively by using 0.3 and 0.05 μm alumina powder and sonicated in ethanol and DI water, respectively, for 5 min. The polished electrode was then dipped in 1% KOH solution for 5 min to generate hydroxyl groups on its surface. Three microliters of 2% APTES were drop-cast on the BDD electrode, followed by immediate drop-casting of 2 μL of GOx (10 mg mL^{-1}) and 2 μL of glutaraldehyde (2%). The cross-linked enzyme layer was dried at RT for 1 h and washed with 0.01 M neutral PBS. To achieve a broad linearity and a dynamic range for the glucose detection, the GOx-X-APTES/BDD electrode was drop-cast with 3 μL of 0.5% Nafion, and the resultant layer was dried at RT for 10 min and washed extensively with 0.01 M PBS to form Nafion/GOx-X-APTES/BDD. This procedure was also used for preparation of a GOx-X-APTES-modified glassy carbon (GC) electrode (3 mm diameter, Shanghai Chenhua Instrument, CHI, China), an X-APTES/BDD electrode, a GOx-X/BDD electrode, a GOx-APTES/BDD electrode (i.e., enzyme electrode without cross-linking with glutaraldehyde), an FAD-X-APTES/BDD electrode, and a FAD-GOx-APTES electrode for comparisons.

Direct Electrochemistry of GOx and Analytical Performance of the Enzyme Electrode. To investigate the DET characteristics and the bioelectrocatalytic performance of the immobilized GOx, the GOx-X-APTES/BDD electrode with and without Nafion coating was subjected to cyclic voltammetry (CV) experiments at various scan rates in neutral PBS. The PBS was nitrogen-saturated, oxygen-saturated, or in ambient air, and supplied without and with different concentrations of glucose. Amperometry was also performed at the applied potential of −0.4 V in both deaerated PBS and PBS under ambient air and provoked with the successive injections of glucose solution to investigate the bioelectrocatalytic activity of GOx and the analytical performance of the enzyme electrode.

RESULTS AND DISCUSSION

Electrode Modification and Enzyme Immobilization. It is challenging to functionalize BDD electrodes to improve their analytical performance without sacrificing their ideal characteristics. The BDD surface was covalently modified with the functional molecule APTES, according to the procedures depicted in Scheme 1. In the first step, the treatment of a BDD

dx.doi.org/10.1021/ac501143e | Anal. Chem. 2014, 86, 4910−4918

Scheme 1. Schematic Illustration for the Chemical Functionalization of the BDD Surface with APTES and GOx by Glutaraldehyde Cross-Linking

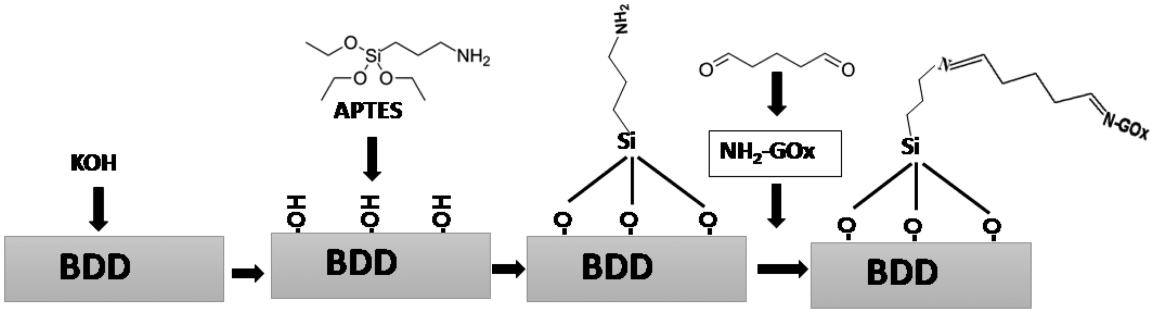

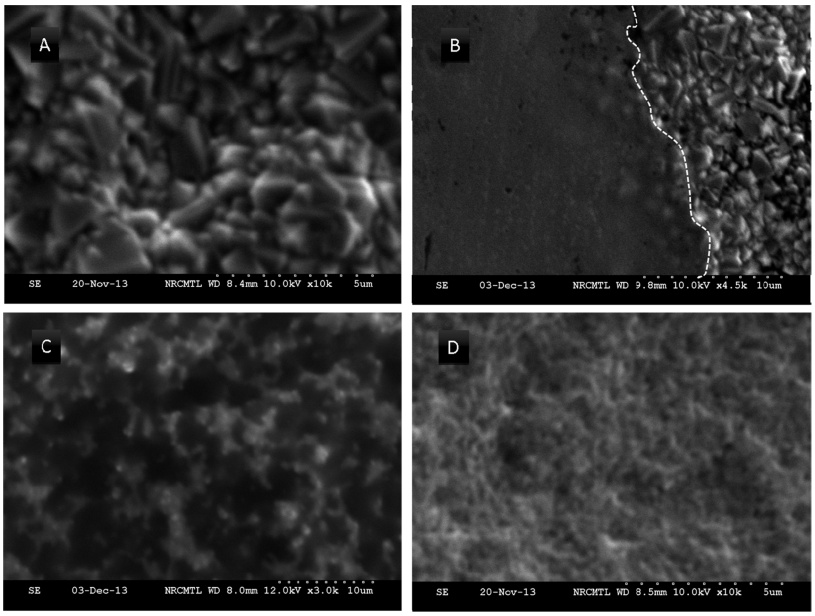

Figure 1. SEM micrographs of (A) pristine BDD; (B) APTES/BDD; (C) X-APTES/BDD with glutaraldehyde to cross-link the amino groups of APTES, and (D) GOx-X-APTES/BDD with glutaraldehyde cross-linking. The white-dashed line in B represents the border between the APTES/BDD (left side) and the pristine BDD (right side).

electrode with the KOH solution resulted in the formation of hydroxyl groups on the BDD electrode. As OH groups can react specifically with different silane derivatives,[22] drop casting of APTES on the KOH-treated BDD surface introduced amine groups to the BDD surface. Upon drop casting of the GOx solution onto the BDD surface, the thereafter introduced glutaraldehyde, a bifunctional chemical, is attacked on its aldehydic carbons by the amino groups of APTES and the amine groups of lysine and FAD of GOx, forming Schiff bases (pink color). The Schiff base formation reaction covalently cross-links GOx (including the FAD center) and APTES, resulting in a stable enzyme layer with an observed pink color on the surface of BDD.

ATR-FT-IR spectroscopy (Figure S-1 of the Supporting Information) was used to confirm the chemical reactions on the surface of the BDD electrode. For the bare BDD electrode, a characteristic peak at 2858 cm^{-1} for the B−C covalent bond is present.[23] When APTES, GOx, and glutaraldehyde were dropped on the surface of the bare BDD electrode, new spectral bands appeared. Bands at 1185 cm^{-1} (OCH_2CH_3) and 1020 cm^{-1} (Si−O−Si) are associated with the bound APTES, which introduces amine groups to the BDD surface.[21] Functionalization of BDD with amine groups can serve as a platform for biomolecule immobilization. Several different approaches have been described for the preparation of amine-terminated BDD electrodes using NH_3 plasma treatment or more intensive chemical treatment.[24,25] Of interest is the hydroxyl groups generated on the oxidized BDD by electrochemical oxidation in sulfuric acid.[26] The hydroxyl groups can be modified with APTES for introduction of various functionalities onto the BDD surface (e.g., tyrosinase can be cross-linked with the amino group of APTES to form a tyrosinase-modified BDD electrode).[26] The treatment of BDD with KOH to generate hydroxyl groups is a very effective and rapid wet chemistry procedure.

SEM images show that the typical diamond microcrystalline faceted grains with pronounced grain boundaries basically disappeared with a modifying layer of APTES (Figure 1, panels A and B). The APTES-modified BDD electrode shows a very smooth and homogeneous silane layer that completely covers the morphology and the characteristically faceted surface of BDD. The presence of small, submicrometer-sized pores was attributed to the drying process even when the drying was performed in an ambient environment. If the APTES-modified BDD surface was treated with glutaraldehyde without the enzyme, surface topography significantly changed with

dx.doi.org/10.1021/ac501143e | Anal. Chem. 2014, 86, 4910−4918

increased roughness and porosity throughout the electrode surface (Figure 1C). Such a result confirmed the cross-linking of the amino group of APTES by glutaraldehyde (Figure 1C). On the other hand, with the presence of GOx, the GOx-X-APTES/BDD shows a mesoporous surface structure (Figure 1D), produced by cross-linking between APTES and GOx, as well as GOx and GOx. The mesoporous structure should be favorable for the permeation of glucose and other small molecules, facilitating the catalytic reaction by the enzyme.

The changes in chemical compositions with the modification were confirmed by EDX analysis. Three different spots at three different magnifications were analyzed with data averaged. The pristine BDD surface showed the following elements in weight percent: C (96.28), O (3.41), and Si (0.30). Upon the modification with the cross-linked enzyme and APTES layer, the weight percent of Si and O increased to 1.25 (contributed from APTES) and 33.69, respectively. The average nitrogen percentage after the modification was 10.42, whereas the carbon percentage decreased to 54.64.

The surface modification was also characterized by using a CV technique. Figure 2 shows the cyclic voltammograms (CVs)

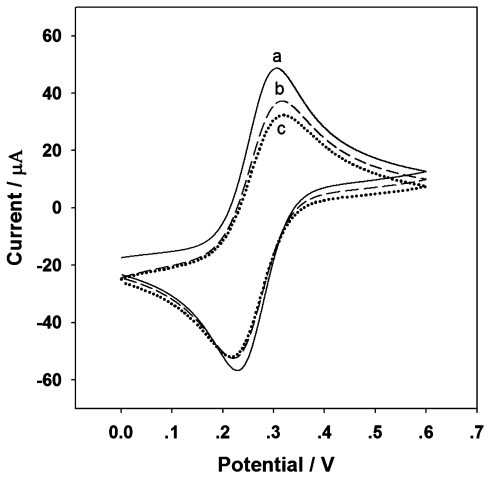

Figure 2. CVs of (a) pristine BDD, (b) BDD treated with KOH (HO-BDD), and (c) APTES-modified BDD (APTES/BDD) with $K_4Fe(CN)_6$ (5 mM) in KCl (1 M) as a redox probe. The scan rate is 0.1 V s^{-1}. In all experiments, CVs were performed immediately after surface pretreatment, thus avoiding the possible modification of consequent surface functional groups by air exposure.

of the pristine BDD, BDD treated with KOH (HO-BDD), and APTES-modified BDD (APTES/BDD) using $K_3Fe(CN)_6$ as a redox probe. The pristine BDD exhibits a well-defined wave with a peak-to-peak potential (ΔE_P) of 77 mV. After KOH treatment and silanization, the CV curve only shows a small attenuation of the peak and insignificant changes in the ΔE_P value. Such a result attested that the silanization of the BDD electrode did not adversely affect its electrical conductivity. The active surface area of the pristine BDD, HO-BDD, and APTES/BDD was estimated to be 0.080, 0.066, and 0.061 cm^2, respectively, using the well-know Randles–Sevcik equation[27,28] (see the Supporting Information). Notice also that $Fe(CN)_6^{4-/3-}$ adsorbed strongly on the salinized BDD as confirmed by the presence of a redox pair from its repeated CVs when the electrode with adsorbed $Fe(CN)_6^{4-/3-}$ is placed back into the blank PBS (Figure S-2 of the Supporting Information). The observed effect could be attributed to the electrostatic attraction between $Fe(CN)_6^{4-/3-}$ and protonated amino groups.

Direct Electrochemistry and Bioelectrocatalysis of GOx. GOx, one of most studied flavoenzymes, is identified by the use of the imbedded enzymatic cofactor FAD. FAD is electroactive and displays a two-electron two-proton redox reaction as $FAD + 2H^+ + 2\ e^- \leftrightarrow FADH_2$. Glucose is oxidized by GOx into D-glucono-1,5-lactone, where two protons and two electrons are transferred from glucose to the GOx cofactor FAD to become $FADH_2$. If the $FADH_2$ can be oxidized back to FAD, resulting in the turning over of GOx without utilization of oxygen or electrochemical mediators, the process is termed as bioelectrocatalysis or DET of GOx. As shown in Figure 3A, in

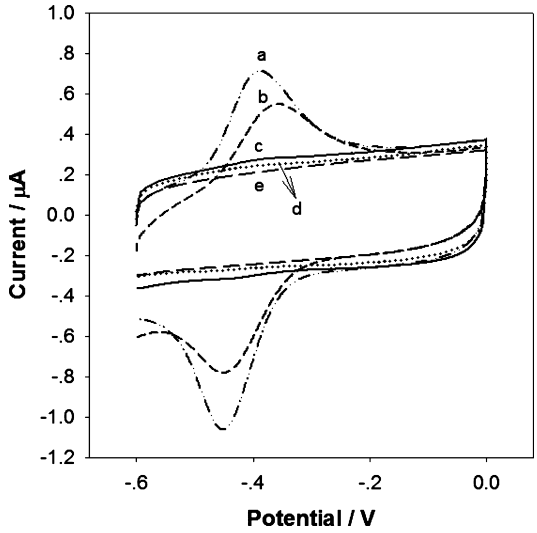

Figure 3. CVs of (a) GOx-X-APTES/BDD, (b) Nafion/GOx-X-APTES/BDD, (c) GOx-APTES/BDD without glutaraldehyde cross-linking, (d) GOx-X/BDD, and (e) X-APTES/BDD electrodes running in nitrogen-saturated 0.01 M PBS (pH 7.0). Scan rate: 0.5 V s^{-1}.

an oxygen-free solution, the CVs of the as-prepared GOx-X-APTES/BDD and Nafion/GOx-X-APTES/BDD in neutral PBS show a pair of well-defined redox peaks, indicating the DET of GOx. For the GOx-X-APTES/BDD electrode, the anodic peak potential (E_{pa}) of the GOx electrochemical reaction is −0.39 V, and the cathodic peak potential (E_{pc}) is −0.45 V, with a formal potential of about −0.42 V, in agreement with the typical electrochemical characteristics of GOx.[29,30] The cathodic peak is attributed to the reduction of FAD to $FADH_2$, while the anodic peak is due to the reversible reoxidization of $FADH_2$ to FAD. With the modification of the Nafion layer, the redox peak current of the enzyme FAD center decreased slightly, accompanied by a slight increase of the ΔE_P value. As expected, the Nafion layer slightly slows down the electron transfer rate of the GOx but does not significantly block it. It should be noted that the cathodic current is appreciably higher than the anodic current at low scan rates. The rationale of such behavior was not clear, but one might expect FAD to undergo a structural change (i.e., the oxidized form is planar versus the butterfly conformation for the reduced form).[31] Without the glutaraldehyde cross-linking step, electrostatic adsorption of GOx on APTES leads to a hardly observable electrode FAD-$FADH_2$ redox reaction, indicating that the glutaraldehyde cross-linking step not only stabilizes the enzyme layer but also reduces the distance between the enzyme

dx.doi.org/10.1021/ac501143e | Anal. Chem. 2014, 86, 4910−4918

redox sites and sensing tips of BDD crystals, as shown in Scheme 1. Similarly, without introduction of APTES, the electrode FAD-$FADH_2$ redox reaction was hardly observable, suggesting that APTES functioned as an electrical wire connecting the GOx redox center to the BDD electrode. APTES molecule has a size of 5−6 Å, whose amino group may be cross-linked with the amino groups of FAD and lysine of GOx through glutaraldehyde. Stable immobilization of free FAD molecules on APTES/BDD through glutaraldehyde cross-linking was proved by stable redox peak current of FAD-$FADH_2$ during repeated CV scanning (Figure S-3 of the Supporting Information), indicating that FAD can be cross-linked with APTES through glutaraldehyde. These results also exclude the possibility that APTES or glutaraldehyde may cause exposure or leakage of FAD from GOx. The GOx cofactor FAD tightly binds to the apoenzyme. The dissociation constant of GOx (i.e., FAD dissociates from holoenzyme forming apoenzyme) is 1.3×10^{-10} M, much smaller than that of D-amino acid oxidase, whose dissociation constant is about 1.2×10^{-7} M.[32] On the other hand, the GOx-X-APTES/GC electrode did not exhibit the redox peaks of GOx (data not shown), suggesting that the surface morphology and/or the chemical composition of the BDD contributes to the DET of GOx for the GOx-modified BDD electrode. The catalytic function of GOx depends not only on the flavin coenzyme but also on other residues at the active site. The influence of the enzyme environment on the chemically active residues is also an important factor for the function. Proteins adsorb and may polymerize on metal electrode surfaces.[33] As an example, lysozyme adsorbed on gold electrodes produces surface-induced conformational changes, which decrease as the polarity of the surface increases.[34] BDD presents an inert surface, which is resistant to deactivation of activity of proteins/enzymes.[35,36] Modification of APTES greatly improves the hydrophilicity of the BDD surface, a favorable factor for keeping the natural conformation of GOx.

The scan rate effect on the direct electrochemical reaction of the immobilized GOx at the Nafion/GOx-X-APTES/BDD and GOx-X-APTES/BDD electrode was investigated. The CVs at the Nafion/GOx-X-APTES/BDD electrode are illustrated in Figure 4A. The linear increase of cathodic peak current (I_{pc}) and anodic peak current (I_{pa}) with increasing scan rate from 0.2 to 4.0 V s^{-1} (as shown in Figure 4B) confirms excellent redox reaction of the FAD/$FADH_2$ couple on BDD as a surface-controlled electrochemical process. A similar result was obtained for the GOx-X-APTES/BDD electrode (Figure S-4 of the Supporting Information). Such behavior can be described by the well-known Laviron equation for determination of the cathodic transfer coefficient (α) and the heterogeneous electron transfer rate constant (k).[37] The linear plots of E_{pa} and E_{pc} versus log ν (ν: scan rate) for the Nafion/GOx-X-APTES/BDD are shown in the inset of Figure 4B, where $\Delta E_p > 200/n$ mV (n represents the number of electrons per molecule oxidized or reduced; for GOx, $n = 2$). From the slopes of E_{pa} and E_{pc} versus log ν (0.073 and −0.074, respectively), the value of α can be determined to be 0.497. Detailed information for the estimation is described in the Supporting Information. Thereafter, the k value was calculated from the Laviron equation (eq 1), by estimating at different scan rates and taking the averaged value.

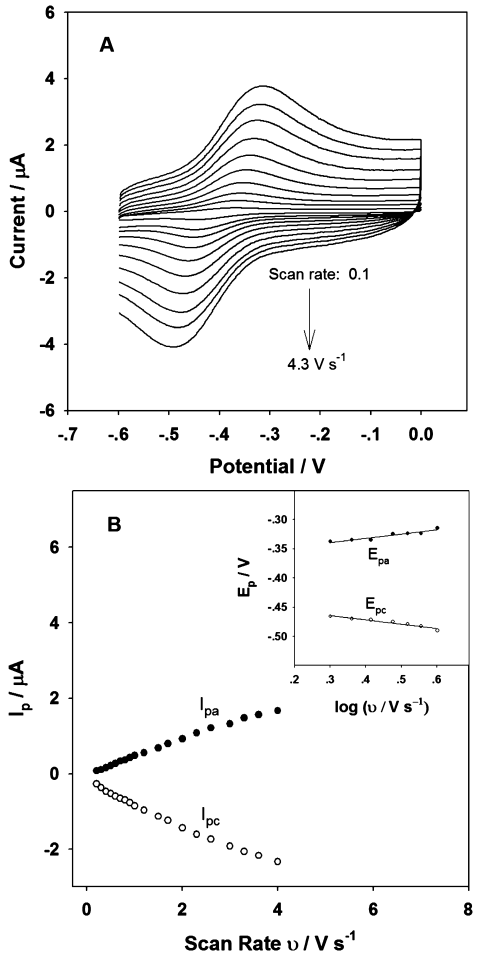

Figure 4. (A) CVs of a Nafion/GOx-APTES BDD electrode in nitrogen-saturated 0.01 M PBS (pH 7.0) at different scan rates ranging from 0.1 to 4.3 V s^{-1}. (B) Plots of the CV peak current (I_p) versus the scan rate (ν). Inset in B: plots of the peak potential (E_p) vs log ν, when $\Delta E_p > 100$ mV.

$$\log k = \alpha \log(1-\alpha) + (1-\alpha)\log \alpha - \log\left(\frac{RT}{nF\nu}\right) - \frac{\alpha(1-\alpha)nF\Delta E_p}{2.3RT} \quad (1)$$

In eq 1, F, R, and T represent Faraday constant (96485.34 C mol^{-1}), gas constant (8.314 J mol^{-1} K^{-1}), and absolute temperature (K), respectively. For the direct electrochemistry of the immobilized GOx, the k value was estimated to be 8.85 ± 0.47 s^{-1}, considerably higher than the literature values observed for GOx biosensors using carbon nanotubes (1.78 s^{-1}; 1.61 s^{-1})[29] or gold nanoparticles (1.69 s^{-1}).[30]

CVs of a Nafion/GOx-X-APTES/BDD electrode at the scan rate of 0.3 V s^{-1} in a blank PBS and a PBS containing 1 mM glucose are shown in Figure 5A. Both testing solutions were deaerated by bubbling with N_2 for more than 30 min and then maintaining a nitrogen blanket over the solution. With the addition of glucose, the FAD reduction peak current decreased obviously, accompanied by an obvious increase in the FADH oxidation current. This result confirms the bioelectrocatalytic activity of the electrical contacted GOx. In the presence of glucose, glucose is oxidized by GOx in concurrence with the biochemical reduction of the GOx FAD to $FADH_2$. The biochemical product $FADH_2$ can be oxidized back to FAD by

dx.doi.org/10.1021/ac501143e | Anal. Chem. 2014, 86, 4910−4918

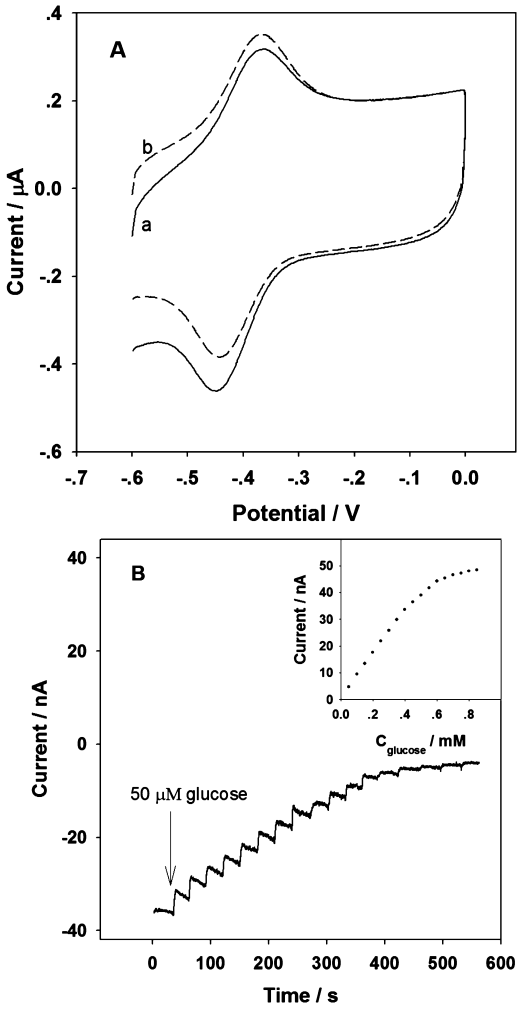

Figure 5. (A) CVs of a GOx-X-APTES/BDD electrode in (a) nitrogen-saturated blank neutral PBS and (b) neutral PBS containing 1 mM glucose. Scan rate: 0.3 V s^{-1}. (B) The amperometric response of a GOx-X-APTES/BDD electrode to successive injections of 50 μM glucose in oxygen-free neutral PBS at the applied potential of −0.40 V. Inset in B: the plot of the amperometric response current versus glucose concentration ($C_{glucose}$).

the electrochemical reaction, resulting in the changes in the GOx FAD redox peak currents, also the GOx turning over for bio-oxidizing another glucose molecule.

Bioelectrocatalytic activity of the electrical contacted GOx was also proved by amperometric glucose response. As the N_2-purged glucose solution was injected into the oxygen-free PBS, a strong increase in the anodic current was observed when the electrode was poised at −0.40 V (Figure 5B). In the absence of oxygen, the glucose response could only be attributed to bioelectrocatalytic oxidation of glucose by the electrically contacted GOx, whose $FADH_2$ is oxidized to FAD by the underlying BDD electrode, resulting in the turning over of GOx. The linear range of the amperometric glucose response is from 15 to 400 μM, and the dynamic range is up to 700 μM. The lower detection limit is 10 μM (signal-to-noise ratio S/N = 3), and the response time is within 5 s. The bioelectrocatalytic enzyme reaction to glucose follows the Michaelis−Menten kinetics. A linear $1/I_{cat}$ versus $1/C_{glucose}$ plot (I_{cat} and $C_{glucose}$ represents the amperometric response current and the glucose concentration, respectively) was obtained with a regression coefficient (R) value of 0.9996, and the apparent Michaelis−Menten constant was obtained to be 491 μM. To further exclude a possible mechanism that the glucose response may be due to FAD molecules leaked from GOx, control experiments for the BDD electrode modified with APTES, GOx, and free FAD molecules (absence of glutaraldehyde) were performed. For this control electrode, although redox peaks from the electrochemical redox reaction of free FAD molecules were clearly observed in deaerated PBS, no obvious amperometric signal toward glucose was observed with the absence of O_2 (Figure S-5 of the Supporting Information).

On the basis of such findings, efficient DET has been realized simply by cross-linking of GOx and APTES with glutaraldehyde on the BDD electrode. An outmost layer of Nafion film coated on the enzyme membrane does not block the direct electrochemical reaction of the GOx FAD center. This finding was somewhat surprising because the redox-active cofactor (FAD) of GOx is buried deeply within the protein core, rendering it inaccessible for direct communication with the electrode surface, which has been achieved by utilization of nanomaterials[1−4,7,8] or surrounding redox polymers.[5,6]

Oxygen Effect. At the ambient environment, most liquids contain some amount of dissolved oxygen (<0.4 mM), which may affect the DET reaction of GOx and the glucose sensing at negative potentials. For DET of GOx FAD center, oxygen can oxidize the GOx ($FADH_2$), enabling the enzyme to be rapidly turned over for an oxygen-catalyzed cathodic reaction.

For the Nafion/GOx-X-APTES/BDD and GOx-X-APTES/BDD electrodes, oxygen exhibited strong catalytic activity toward the reduction of GOx(FAD). Figure 6A compares the CVs of a GOx-X-APTES/BDD electrode in oxygen-saturated, air-saturated, and nitrogen-saturated PBS. A significant increase of the cathodic peak current in the presence of dissolved oxygen is accompanied with a decrease of the anodic peak current, since O_2 will compete with the electrode for $FADH_2$. The mesoporous structure of the GOx-X-APTES layer, as observed from the SEM images, allows the dissolved oxygen molecules access to the immobilized GOx rapidly and efficiently, accelerating the oxidation reaction of $FADH_2$ by oxygen.

The CV signal responses of the Nafion/GOx-X-APTES/BDD and GOx-X-APTES/BDD electrodes to increasing concentrations of glucose were examined in air-saturated and oxygen-saturated PBS. In the presence of oxygen, the cathodic peak current for FAD reduction decreased with the increase of glucose concentration. In contrast, the anodic wave increased as the glucose concentration increased. Figure 6B shows the CVs of a Nafion/GOx-X-APTES/BDD electrode in oxygen-saturated PBS containing different concentrations of glucose. The anodic peak at about −0.40 V became pronounced at the glucose concentrations above 7 mM. Glucose competes with the electrochemical step for FAD, therefore catalyzing the electro-oxidation of $FADH_2$, consistent with the CV experimental results in deaerated PBS. This result again attested the bioelectrocatalytic activity of the electrical contacted enzyme. The significant decrease of the FAD reduction current should also be contributed more or less by the consumption of O_2 from the natural enzymatic glucose oxidation. Although the GOx molecules are efficiently electrically wired by the glutaraldehyde-APTES conjugate molecules (as a very high k value has been determined), they can still keep their natural enzymatic bioactivity. APTES and glutaraldehyde molecules are small, biocompatible, and flexible and would not disrupt the natural conformation of GOx.

dx.doi.org/10.1021/ac501143e | Anal. Chem. 2014, 86, 4910−4918

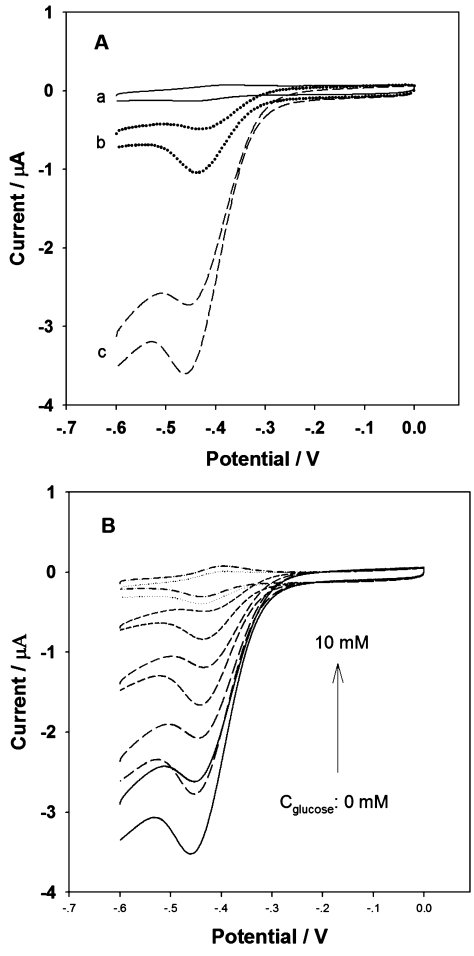

Figure 6. (A) CVs of a GOx-X-APTES/BDD electrode operated in (a) oxygen free, (b) ambient air, and (c) oxygen saturated 0.01 M neutral PBS. (B) CVs of a GOx-X-APTES/BDD electrode operated in oxygen-saturated PBS at increasing glucose concentration ($C_{glucose}$) (0, 1, 3, 5, 7, and 10 mM). Scan rate: 0.1 V s^{-1}.

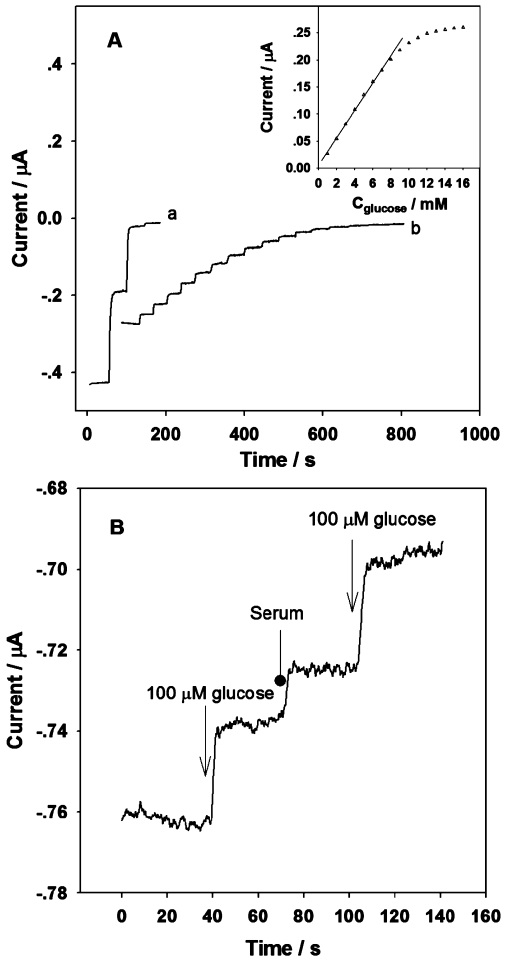

Figure 7. (A) Amperometric spectra of (a) GOx-X-APTES/BDD and (b) Nafion/GOx-X-APTES/BDD electrodes in response to successive injections of 1 mM glucose in neutral PBS at the applied potential of −0.40 V, under an ambient environment. Inset in A: the plot of the amperometric response current at the Nafion/GOx-X-APTES/BDD electrode versus glucose concentration ($C_{glucose}$). (B) The response signal of a Nafion/GOx-X-APTES/BDD electrode poised at −0.40 V to a human serum sample (40 μL) in blank neutral PBS (5 mL) under an ambient environment.

Analytical Performance. The amperometric responses to glucose were performed at −0.4 V, by successively injecting glucose solution into the neutral PBS at ambient environment. As illustrated in Figure 7A and Figure S-6 of the Supporting Information, the GOx-X-APTES/BDD biosensor (curve a in Figure 7A) showed a linear response range from 25 μM to 1.8 mM, with a dynamic range up to 3 mM and a detection limit of 20 μM glucose ($S/N = 3$). Both ascorbic (0.1−1 mM) and uric acids (0.2 mM) at normal physiological levels did not provoke any signal responses. The linear range of glucose sensing is broader than that in deaerated PBS (from 15 to 400 μM), suggesting that oxygen is also involved in the biosensing process. Such results were expected since oxygen can compete with the electrode for the oxidation of $FADH_2$, therefore increasing the FAD turnover rate and the bioelectrocatalytic activity of GOx. The consumption of oxygen by the natural bioactivity of GOx for glucose oxidation will slightly decrease the electro-reduction current of oxygen. The overpotential of oxygen reduction at a BDD electrode is larger than that at a GC electrode in acidic and alkaline solutions.[9,10] The X-APTES/BDD prepared in this work exhibited a slight oxygen reduction current at −0.4 V (Figure S-7 of the Supporting Information).

The response range at the GOx-X-APTES/BDD biosensor is comparable to 0.5−3.5 mM for GOx on reduced graphene oxide and gold−palladium bimetallic nanoparticle-modified GC electrodes.[38] In consideration of the range of normal blood glucose (4.4−6.6 mM) and the diabetic blood glucose (up to 32 mM) concentrations, it would be more ideal for practical applications to have an even broader range of dynamic response. As shown in Figure 7A, the dynamic range was noticeably improved by drop-casting a thin layer of Nafion on the GOx-BDD surface. The linear range of glucose response at the Nafion/GOx-X-APTES/BDD biosensor (curve b in Figure 7A) was from 35 μM to 8.0 mM, with a regression coefficient of 0.9983 and a lower detect limit of 30 μM ($S/N = 3$). The response time was within 5 s, and the dynamic range was up to 14 mM of glucose concentration. At high glucose levels, the Nafion film serves as a glucose-limiting membrane to prevent the enzyme from reacting with the excessive glucose molecules. Nafion film can also act as an anti-interference membrane to prevent the diffusion of electro-active interferents and drug metabolites to the electrode surface.

The Nafion/GOx-X-APTES/BDD electrode was reused for over 100 repetitive injections of glucose at varying concen-

dx.doi.org/10.1021/ac501143e | Anal. Chem. 2014, 86, 4910−4918

tration (100 μM to 1 mM). The response signals did not show obvious diminishing after the detections, attesting the operational stability of the enzyme electrode. GOx is a very stable and specific enzyme with operational and storage stability well-documented in the literature. The covalent bonding between APTES and BDD, the cross-linking step, and the Nafion coating together, prevent the leaching/detaching of the immobilized enzyme. In addition, our experimental data confirmed that after 2 weeks of storage in sterilized PBS at 4 °C, the Nafion/GOx-X-APTES/BDD electrode retained its original response sensitivity.

The biosensor was then evaluated for applications in physiological human serum samples. The human serum sample was obtained from the School Hospital of Zhengzhou University. The biosensor was used to determine the glucose level in the sample, and the matrix effect of the physiological sample on the biosensor was investigated. For each amperometric measurement, the blank neutral PBS (5 mL) was spiked first with 100 μM of standard glucose, followed by one injection of 40 μL of human serum, and finally with another 100 μM of standard glucose (Figure 7B). The recovery rate of the glucose level for the second standard injection is 104%, indicating that the physiological sample does not put an obvious matrix effect on the biosensor. The Nafion film coated on the surface of the biosensor should be able to improve the antifouling effect of the enzyme electrode. The glucose level in the human serum sample was determined to be 6.1 mM, falling into the range for healthy people.

CONCLUSIONS

In brief, this work demonstrates the feasible achievement of efficient DET using a BDD electrode and a simple enzyme immobilization procedure with GOx as a test model. To our knowledge, this is the first time that DET of GOx based on APTES and BDD has been demonstrated. The proposed glucose biosensor can be prepared by a facile and rapid procedure without expensive reagents and complicated experiments. Physiological levels of interferents do not present any signals at the glucose biosensor. This glucose biosensor is stable, sensitive, precise, fast-responding, and exhibits a broad linear range. It can work under both deaerated and aerated environments. Human serum matrix does not affect the performance of the biosensor. This approach holds great promises for applications in third-generation biosensors or as anodes in enzyme-based biofuel cells.

ASSOCIATED CONTENT

Supporting Information

Additional information as noted in text. This material is available free of charge via the Internet at http://pubs.acs.org.

AUTHOR INFORMATION

Corresponding Author

*E-mail: hfcui@zzu.edu.cn. Tel: +86-371-67781325. Fax: +86-371-67783235.

Notes

The authors declare no competing financial interest.

ACKNOWLEDGMENTS

This work was financially supported by the National Natural Science Foundation of China (NSFC 21345007), the National Recruitment Program of High-End Foreign Experts (China, GDW20124100167), and the Scientific Research Foundation for the Returned Overseas Scholars from Ministry of Human Resources of China. We thank Sabahudin Hrapovic and Edmond Lam from National Research Council Canada who did the SEM and FT-IR measurements and Ai-Wei Zhou from Zhengzhou University who did some routine lab work.

REFERENCES

(1) Guiseppi-Elie, A.; Lei, C.; Baughman, R. H. *Nanotechnology* **2002**, *13*, 559−564.
(2) Cui, H. F.; Zhang, K.; Zhang, Y. F.; Sun, Y. L.; Wang, J.; Zhang, W. D.; Luong, J. H. T. *Biosens. Bioelectron.* **2013**, *46*, 113−118.
(3) Shan, C. S.; Yang, H. F.; Song, J. F.; Han, D. X.; Ivaska, A.; Niu, L. *Anal. Chem.* **2009**, *81*, 2378−2382.
(4) Liang, B.; Fang, L.; Yang, G.; Hua, Y. C.; Guo, X. S.; Ye, X. S. *Biosens. Bioelectron.* **2013**, *43*, 131−136.
(5) Degani, Y.; Heller, A. *J. Phys. Chem.* **1987**, *91*, 1285−1289.
(6) Wang, J. *Chem. Rev.* **2008**, *108*, 814−825.
(7) Katz, E.; Sheeney-Haj-Ichia, L.; Willner, I. *Angew. Chem., Int. Ed.* **2004**, *43*, 3292−3300.
(8) Holland, J. T.; Lau, C.; Brozik, S.; Atanassov, P.; Banta, S. *J. Am. Chem. Soc.* **2011**, *133*, 19262−19265.
(9) Yano, T.; Tryk, D. A.; Hashimoto, K.; Fujishima, K. *J. Electrochem. Soc.* **1998**, *145*, 1870−1876.
(10) Yano, T.; Popa, E.; Tryk, D. A.; Hashimoto, K.; Fujishima, A. *J. Electrochem. Soc.* **1999**, *146*, 1081−1087.
(11) Xu, J.; Granger, M. C.; Chen, Q.; Strojek, J. W.; Lister, T. E.; Swain, G. M. *Anal. Chem.* **1997**, *69*, 591A−597A.
(12) Jolley, S.; Koppang, M.; Jackson, T.; Swain, G. M. *Anal. Chem.* **1997**, *69*, 4099−4107.
(13) Luong, J. H. T.; Male, K. B.; Glennon, J. D. *Analyst* **2009**, *134*, 1965−1979.
(14) Spataru, N.; Tokuhiro, K.; Terashima, C.; Tao, T. N.; Fujishima, A. *J. Appl. Electrochem.* **2003**, *33*, 1205−1210.
(15) McCreery, R. L. *Chem. Rev.* **2008**, *108*, 2646−2687.
(16) Troup, C. E.; Drummond, I. C.; Graham, C.; Grice, J.; John, P.; Wilson, J. I. B.; Jubber, N. G.; Morrison, N. A. *Diamond Relat. Mater.* **1998**, *7*, 575−580.
(17) Tatsuma, T.; Mori, H.; Fujishima, A. *Anal. Chem.* **2000**, *72*, 2919−2924.
(18) Rao, T. N.; Yagi, I.; Miwa, T.; Tryk, D. A.; Fujishima, A. *Anal. Chem.* **1999**, *71*, 2506−2511.
(19) Shang, F. J.; Glennon, J. D.; Luong, J. H. T. *J. Phys. Chem. C* **2008**, *112*, 258−29263.
(20) Yu, Y.; Zhou, Y. L.; Wu, L. Z.; Zhi, L. F. *Int. J. Electrochem.* **2012**, *2012*, 567171−567181.
(21) Zheng, D.; Vashist, S. K.; Al-Rubeaan, K.; Luong, J. H. T.; Sheu, F. S. *Analyst* **2012**, *137*, 3800−3805.
(22) Li, H. S.; Qi, Y. X.; Gong, J. H.; Wang, M.; Li, M. S. *Int. J. Refract. Met. Hard Mater.* **2009**, *27*, 564−570.
(23) Vandenberg, E. T.; Bertilsson, L.; Liedberg, B.; Uvdal, K.; Erlandsson, R.; Elwing, H.; Lundström, I. *J. Colloid Interface Sci.* **1991**, *147*, 103−118.
(24) Yang, W.; Auciello, O.; Butler, J. E.; Cai, W.; Carlisle, J. A.; Gerbi, J. E.; Gruen, D. M.; Knickerbocker, T.; Lasseter, T. L.; Russell, J. N.; Smith, L. M.; Hamers, R. J. *Nat. Mater.* **2002**, *1*, 253−257.
(25) Yang, W. S.; Baker, S. E.; Butler, J. E.; Lee, C. S.; Russell, J. N.; Shang, L.; Sun, B.; Hamers, R. J. *Chem. Mater.* **2005**, *17*, 938−940.
(26) Notsu, H.; Tatsuma, T.; Fujishima, A. J. *Electroanal. Chem.* **2002**, *523*, 86−92.
(27) Randles, J. E. B. *Trans. Faraday Soc.* **1952**, *48*, 828−832.
(28) Bard, A. J.; Faulkner, L. R. *Electrochemical Methods: Fundamentals and Applications*, 2nd ed.; John Wiley & Sons: New York, 2001.
(29) Zhao, Y. D.; Zhang, W. D.; Chen, H.; Luo, Q. M. *Anal. Sci.* **2002**, *18*, 939−941.
(30) Wu, Y. H.; Hu, S. S. *Bioelectrochemistry* **2007**, *70*, 335−341.

(31) Birss, V. I.; Elzanowska, H.; Turner, R. A. *Can. J. Chem.* **1988**, *66*, 86−96.
(32) Okuda, J.; Nagamine, J.; Kunio, Y. *Biochim. Biophys. Acta* **1979**, *566*, 245−252.
(33) Lehrer, S. S.; Fasman, G. D. *Biochemistry* **1967**, *6*, 757−767.
(34) Kleijn, J. M.; Barten, D.; Stuart, M. A. C. *Langmuir* **2004**, *20*, 9703−9713.
(35) Watanabe, T.; Ivandini, T. A.; Makide, Y.; Fujishima, A.; Einaga, Y. *Anal. Chem.* **2006**, *78*, 7857−7860.
(36) Suzuki, A.; Ivandini, T. A.; Yoshimi, K.; Fujishima, A.; Oyama, G.; Nakazato, T. *Anal. Chem.* **2007**, *79*, 8608−8615.
(37) Laviron, E. *J. Electroanal. Chem.* **1979**, *101*, 19−28.
(38) Yang, J.; Deng, S. Y.; Lei, J. P.; Ju, H. X.; Gunasekaran, S. *Biosens. Bioelectron.* **2011**, *29*, 159−166.